ARCHIVES OF ELECTRICAL ENGINEERING VOL. 69(2), pp. 249–258 (2020)

DOI 10.24425/aee.2020.133023

Influence of rotor's cage resistance on demagnetization process in the line start permanent magnet synchronous motor

TOMASZ ZAWILAK

Department of Electrical Machines, Drives and Measurements
Wroclaw University of Science and Technology
Wroclaw, Poland
e-mail: tomasz.zawilak@pwr.edu.pl

(Received: 24.02.2019, revised: 16.12.2019)

Abstract: This paper deals with the finite element analysis of the demagnetization process of the line start permanent magnet synchronous motor. Special attention has been paid to demagnetization risk assessment after resynchronization during a short-term supply power outage. The current and torque waveforms have been determined assuming the difference depending initial rotor position angle. It has been demonstrated that the highest demagnetization risk occurs when resynchronization (motor reclosing) is performed when induced electromotive forces are in anti-phase to the supply voltage waveforms. The effect of cage winding resistance on the risk of demagnetization is examined and discussed.

Key words: demagnetization, falling out of step, permanent magnets, synchronous motor

1. Introduction

Due to the development of permanent magnets of a high energy product, the Line Start Permanent Magnet Synchronous Motors (LSPMSMs) have become an alternative to the conventional squirrel cage induction motors. The main advantages of the LSPMSM are: high efficiency (an efficiency class as high as IE5) and a high power factor. However, the troublesome starting and the risk of demagnetization of the permanent magnets limit a more widespread use of the LSPMSMs. Initially, it was thought that the highest demagnetization risk occurs in the first phase of the starting process (shorting), because of a high inrush current value [1, 2]. In practice, the stator current is a reaction to the high current induced in the starting cage winding. Actually, this induced current screens and reduces the field which could demagnetize the magnets, whereby

the resultant demagnetizing magnetomotive force is relatively small. In the author's opinion a much more hazardous situation occurs if the motor is switched to full voltage when the rotor speed is close to the synchronous one. Due to negligible slip value, the shielding effect of the cage winding is insufficient to protect the magnets against a high armature reaction field. Such a situation is not a theoretical case used to study the worst scenario but can happen in reality during the operation of an LSPMSM drive, for example, during a momentary voltage collapse, when after a short-term power outage the voltage is rebuilt [3–5]. The phenomena occurring in the LSPMSM drive in the described above conditions have not been investigated in detail in the literature on the subject. The aim of the conducted research was to investigate the phenomena which can result in the demagnetization of the permanent magnets in the LSPMSM during its reclosing.

2. Model of the LSPMSM

The field-circuit model of the studied machine was implemented in the professional finite element method (FEM) package Ansys Maxwell. The planar symmetry of the magnetic field in the studied machine was assumed. To study the machine performance and permanent magnet (PM) demagnetization risk under voltage excitation, the time stepping algorithm was used to represent time derivatives in the model. The applied field-circuit model consists of two mutually coupled parts: a field part and a circuit part.

In each time step both magnetic field equations and electrical equations are solved for the circuit part. On the basis of the magnetic field solution, one can determine the voltages constituting the sources of the electromotive force in the circuit part equations. The circuit part solution consists of the values of the currents being the source of the magnetic field in the field part's next calculation step.

The sought magnetic field distribution is determined by solving Ampere's law and expressing the magnetic flux density vector by the circulation of the magnetic vector potential $\boldsymbol{A}$:

$$rot\,(\nu \cdot rot\,\boldsymbol{A}) = \boldsymbol{J}_t\,, \tag{1}$$

where: $\boldsymbol{J}_t$ and $\boldsymbol{A}$ are the total current density and magnetic vector potential, respectively, and ν is the reluctivity.

The total current density vector $\boldsymbol{J}_t$ describes all sources of the magnetic field in the considered system taking into account eddy currents induced due to the time variation of the magnetic field and the velocity of the conductive parts as well as magnetization currents expressing the presence of the permanent magnet in the system. For a 2D approach and formulation using the electric scalar potential V

$$\boldsymbol{J}_t = \boldsymbol{J}_o - \sigma\left(grad\,V + \frac{\partial \boldsymbol{A}}{\partial t} + v \times rot\,\boldsymbol{A}\right) + rot\,\boldsymbol{H}_c\,, \tag{2}$$

where: σ is the conductivity, V is the electrical scalar potential, v is the velocity of the conductive elements relative to the magnetic flux density B and $\boldsymbol{H}_c$ is the coercivity of the regions of the permanent magnets.

In each time step the electromagnetic torque acting on the motor rotor is determined from the virtual-work-principle relation:

$$T_B = \frac{\mathrm{d}W(\vartheta, i)}{\mathrm{d}\vartheta}, \tag{3}$$

where: W is the magnetic coenergy of the system, as a function of the current (i) and ϑ is the rotor angular position.

In the presented studies on the demagnetization process of an LSPMSM, it was assumed that the rotational speed of the rotor was constant. Neglecting the mechanical equilibrium equation of the movable elements allowed one to significantly shorten the calculation time while the initially performed research showed that the inclusion of a dynamic equation for high inertial loads did not significantly affect the demagnetization phenomena. As mentioned above, the model of the studied LSPMSM was implemented in the Ansys Maxwell 2D (v. 15) professional FEM package. The structure of the magnetic circuit of the studied machine as well as the view of the applied FE mesh are shown in Fig. 1. Despite the symmetry of the magnetic circuit, the considered domain was intentionally left unreduced, in respect to the original geometry, for a more natural visualisation of the magnetic field distribution. Also, due to the assumption of the planar symmetry, the proper formulations of the end rings of the rotor cage winding as well as the stator end winding were imposed. The rated parameters of the studied machine and major dimensions of its magnetic circuit are summarized in Table 1.

Table 1. Rated parameters and major dimensions of the motor

Shaft power (P_n)	kW	45
Speed (n_n)	rpm	1500 (4 poles)
Torque (T_n)	N·m	286
Voltage (U_n)	V	400
Current (I_n)	A	68.3
Power factor ($\cos\varphi_n$)	–	0.98
Efficiency (h_n)	%	96.9
Starting current (I_r/I_n)	see Fig. 3	
Starting torque (M_r/M_n)	see Fig. 3	
Stator outer diameter	mm	368
Rotor outer diameter	mm	228
Air-gap length	mm	2.5
Core length	mm	220
Permanent magnets (N42 SH)	mm	35×8

It was adopted that the sintered rare earth NdFeB permanent magnet of grade N42SH would be used in the motor. The family of the demagnetization characteristics of the N42SH material at different operating temperatures is shown in Fig. 2.

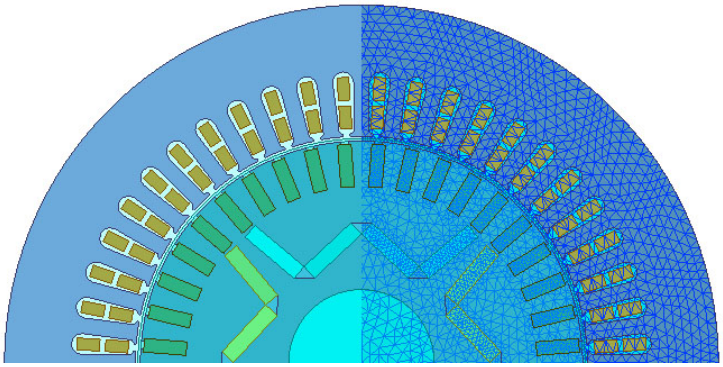

Fig. 1. Geometry and applied FE mesh of the field model of LSPMSM

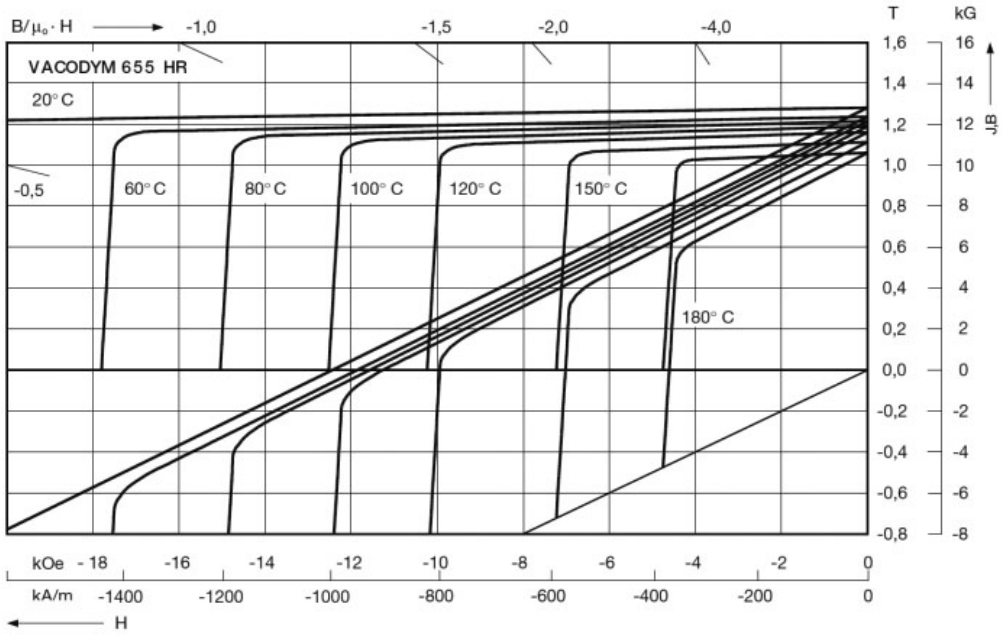

Fig. 2. Demagnetization curves of the N42SH permanent magnets

3. Results of the investigations

One of the difficulties and challenges related to the design of an LSPMSM is to ensure the proper synchronization of the motor. During the starting process, the flux of the permanent magnets generates a braking torque which reduces the resultant asynchronous torque produced by the cage winding, this phenomenon is especially observable at the low range of rotational speeds of the rotor. One of the ways to mitigate this problem is increasing the resistance of the cage,

whereby the breakdown slip shifts towards lower rotor speeds and, consequently, the starting torque increases [6, 7]. However, it should be noted that lowering the value of the breakdown slip will reduce also the "pull in" torque and can lead to a failure of the synchronization process of the motor for high inertia loads [8]. In other words, such an approach will be an effective and safe solution when the moment of inertia of the drive is low (e.g. motor is driving a pump). It is also advisable to increase the resistance of the rotor cage in the case of the LSPMSMs in which a stator winding of a different number of pole pairs than in the rotor is used [9, 10]. In such solutions the resistance of the cage is intentionally increased during a design process to decrease the starting current value. Affecting the cage winding resistance (in both manners, either by the change of the material of different conductivity or the change of a cross-section and/or the shape of the bars), besides profiling, the starting properties of the LSPMSM have an impact on the demagnetization process. To illustrate the above discussed aspects the influence, cage winding material conductivity was examined first.

A. Effect of cage winding material conductivity on the starting properties of the motor

As mentioned above, the cage winding resistance can be varied during the design process by adjusting the slot cross-section and/or by changing the material of the cage. For the purpose of the studies presented in this paper, the geometry of the rotor was intentionally left unchanged so as not to introduce additional factors in the analysis of the starting process and demagnetization risk. At the first stage, the influence of the cage winding conductivity σ on the starting current and the steady state torque vs. speed characteristics was examined. The analysis was performed for the rotor cage windings made of materials of different conductivities. The corresponding materials are: copper (σ = 48 MS/m), brass (σ = 12 MS/m), phosphor bronze (σ = 6 MS/m) and silicon bronze (σ = 3 MS/m).

The determined steady state electromagnetic torque and starting currents vs. speed characteristics for the studied cage winding materials are shown in Fig. 3(a) and Fig. 3(b), respectively.

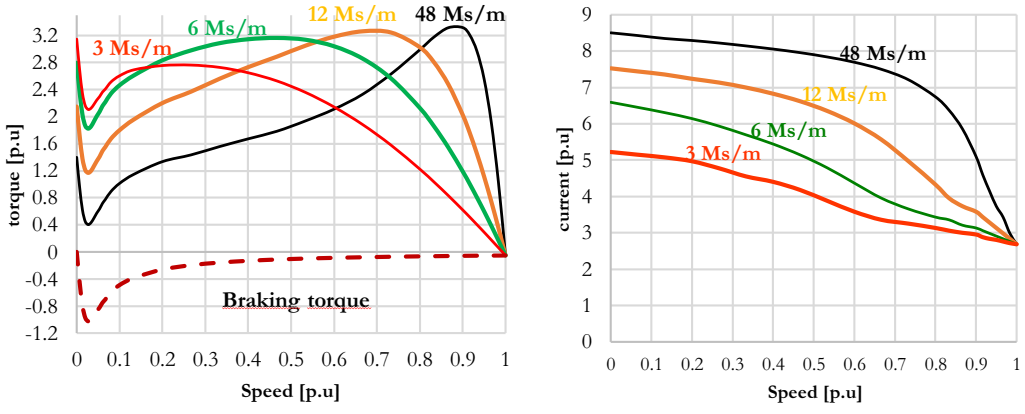

(a) (b)

Fig. 3. Characteristics of: steady-state of electromagnetic torque (a) and current (b) for different materials of the rotor cage winding

To determine the value of the steady state electromagnetic torque, the approach discussed in [11] was applied. The asynchronous component $T_a(n_r)$ of the steady state electromagnetic torque was determined first. It was assumed that rotor speed n_r is forced and permanent magnets were replaced by the material with vacuum-like magnetic properties. Rotor speed n_r was a parameterized form of 0 to synchronous speed n_s with step Δn equal to 50 rpm. Due to the magnetic asymmetry in axes "d" and "q" of the LSPMSM and presence of the parasitic torques, the period of the asynchronous torque waveforms differed from the supply voltage period and depended also on the rotational speed. The resultant asynchronous component of the steady state electromagnetic torque was calculated as the average value of the steady state torque waveform, while the periodicity of the torque waveform was determined individually for each n_r value. Next, braking torque $T_b(n_r)$, generated by the magnets, was determined by modelling a state similar to that of a synchronous machine operating individually with short-circuited windings

The value of $T_b(n_r)$ was calculated as the average value of the electromagnetic torque waveforms in the steady state, at parametrically set rotor speed n_r. Finally, steady state electromagnetic torque $T(n_r)$ was calculated as $T_a(n_r) + T_b(n_r)$.

As it was expected, the presented results confirm that lowering the value of the cage winding resistance leads to a decrease in the breakdown slip value as well as a decrease in the breakdown toque due to the presence of the braking torque produced by the magnets. On the other hand, the increased value of cage material resistivity allows to reduce the motor rms current during the motor start up. To study the impact of the cage winding resistance on the demagnetization risk during the LSPMSM reclosing, the effect of initial angle δ_i (describing the instant of reclosing) was examined in the next step.

B. Simulations of motor reclosing – the effect of initial angle δ_i

As discussed in the introduction, the resynchronization of the LSPMSM after a short-term power outage, i.e. motor reclosing, can be dangerous for the motor permanent magnets in terms of the demagnetization. In general, for the detailed analysis of the electromagnetic phenomena in the considered conditions, the model of the permanent magnet should include the nonlinear demagnetization characteristic and its dependence on temperature (see Fig. 2). However, taking into account the nonlinear model of the permanent magnet leads to a more complex FE model in terms of the computation time. It should also be noted that such functionality is not commonly implemented in the commercially available FEM packages and requires specialised knowledge and skills from the designer to properly set up the PM model. To mitigate the above discussed issues the simplified method of demagnetization risk assessment was proposed.

In real conditions, when a power outage occurs, the rotor speed will decrease due to the lack of driving torque. However, when the inertia of the load is high and the power outage is of a short-term nature, the drop in the speed will be marginal and thus the value of the induced back electromotive force (*emf*) will be close to the rated value. In such a case returning the power to the machine can occur when induced back *emfs* are not in the same phase in comparison with the supply voltage as before the power collapse. In the paper, to study the impact of the instant of the reclosing on the current and torque waveforms, a simplified approach was proposed. The simulations of the motor reclosing were carried out assuming that the motor rotates at a synchronous speed driving the high inertia load. In such conditions, when the power outage is

assumed to be short-term (about milliseconds), the model does not require taking into account the mechanical equilibrium equation. However, it should be noted that in real conditions the reclosing process has a stochastic character.

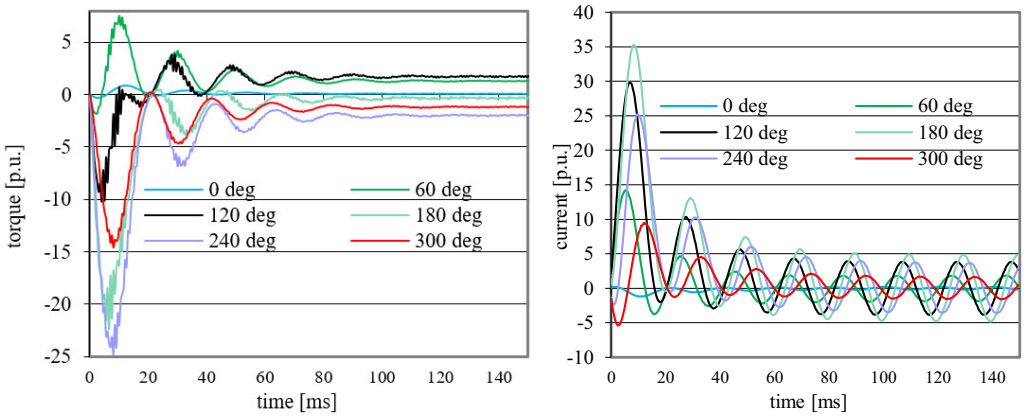

(a) (b)

Fig. 4. Electromagnetic torque: (a) and current waveforms; (b) during motor reclosing for different values of δ_i angle

The instant of the reclosing was represented by electrical angle δ_i between the vector of the induced back *emf's*, by permanent magnets and the supply voltage vector. Depending on the power outage duration, this angle can vary from 0 to 360 degrees. In the proposed approach, due to the imposed simplification regarding the mechanical equilibrium equation, δ_i directly corresponds to the initial mechanical position of the rotor and also determines the internal power angle in a steady state. Nevertheless, for the investigation of the impact of δ_i on demagnetization risk, the maximum inrush current value is most important and should be focused on. The calculated torque and current waveforms for the selected initial angles δ_i are shown in Figs. 4(a) and 4(b), respectively. It appears, especially from the current waveforms that, as expected, the worst case for the motor in terms of the inrush current value is reclosing at δ_i equal to 180°, i.e. it powers up the machine when the corresponding phase electromotive forces induced by the permanent magnets are in an anti-phase to the supply voltages.

It should be also observed that the peak value of the inrush current for the worst case scenario is over 35 times higher than the rated current that is about 4 times higher than the steady state starting current. The effect of rotor cage material conductivity was examined at the subsequent stage of research.

C. Simulations of reclosing – the effect of rotor cage conductivity

To study the impact of cage winding resistance on permanent magnet demagnetization risk, the simulations of motor reclosing in the anti-phase were conducted. Similarly to section A, cage winding materials were studied. The torque and current waveforms calculated during the reclosing

of the motor for four different values of rotor winding conductivity are shown in Figs. 5(a) and 5(b), respectively. The obtained results indicate that cage conductivity has a much stronger effect on the current waveform than on the torque waveform.

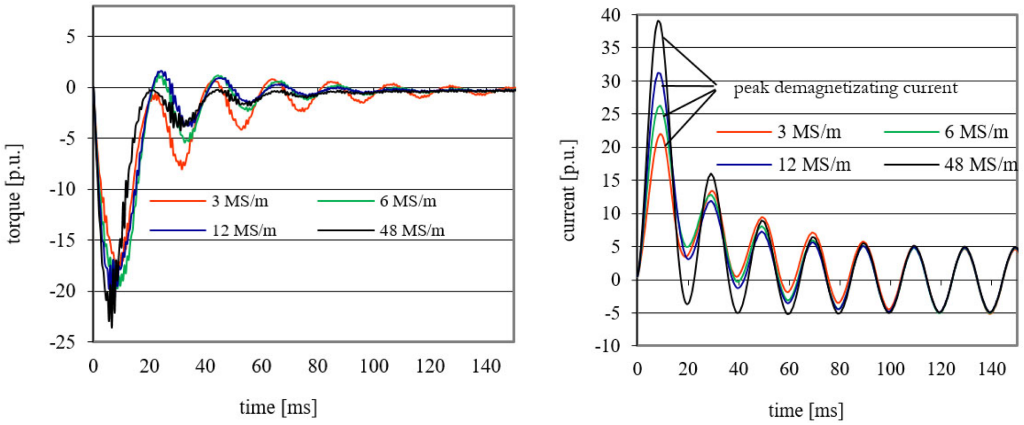

Fig. 5. Torque (a) and phase current (b) waveforms during reclosing (δ_i = 180 deg) for different conductivities of the rotor cage winding material

The peak value of the current occurs in the first half-period of the transient state after reclosing. It can be even up to about 35 times higher than the rated value motor current. The peak inrush current is higher for the lower values of the resistance of the rotor cage winding. In a steady state the current waveform is independent of cage winding resistance, which is logical since the rotor cage currents decay in this operating condition. To assess the risk of permanent magnets demagnetization, the distribution of the magnetic flux density vectors was analysed next. The time instant of the maximum current surge was studied. The distributions determined for the studied cage materials were compared in Fig. 6. Regarding the demagnetization risk assessment, the most important is the distribution of magnetic flux density in the magnets. As it can be seen, for the highest cage conductivity (σ = 48 MS/m) magnetic flux density in the magnets exceeds 0.3 T along the direction of primary magnetization. As material conductivity decreases, flux density (at the studied time instant) in the permanent magnets also decreases, and for the material with a conductivity of 3 MS/m it reaches about 0.2 T (however, in the direction opposite to primary magnetization). This means that at the rotor temperature of about 100°C the magnets would undergo demagnetization (see Fig. 2). It should be noted that the risk of demagnetization increases with the resistance of the cage winding due to the weakening of its shielding effect and not directly with the value of the peak current. It can be observed that in the case illustrated in Fig. 6(a) (the cage winding material of σ equal to 48 MS/m) is characterized by the highest current surge (Fig. 4) and at the same time, by the lowest magnet demagnetization risk.

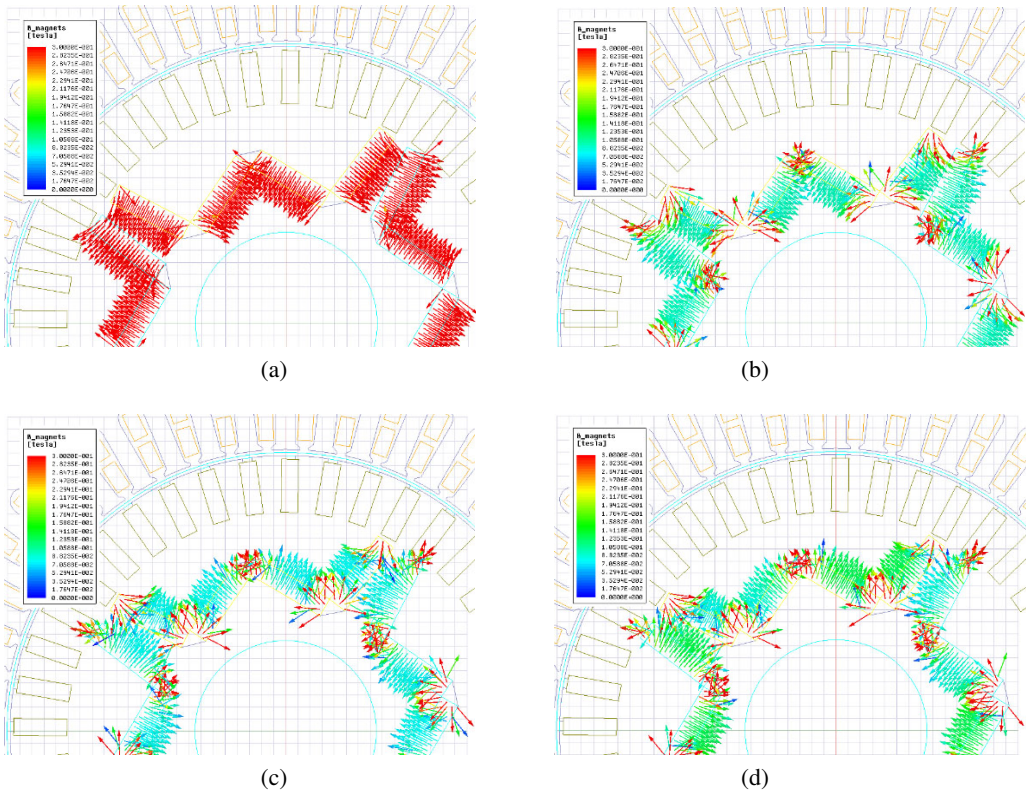

(a) (b)

(c) (d)

Fig. 6. Distribution of magnetic flux density vectors at the highest demagnetizing current for conductivities of the rotor cage winding equal to: (a) 48 MS/m; (b) 12 MS/m; (c) 6 MS/m; (d) 3 MS/m (black arrows indicate the direction of primary magnetization)

4. Conclusion

The demagnetization risk of the line start permanent magnet synchronous motor was assessed by means of the finite element analysis. Special attention was paid to the demagnetization risk assessment and resynchronization during a short-term supply power outage. A simplified and effective method of the demagnetization risk assessment during the reclosing process was proposed as a result. It was demonstrated that the highest demagnetization risk occurs when resynchronization (motor reclosing) is performed when the induced electromotive forces are in anti-phase to the supply voltage waveforms. The effect of the cage winding resistance on the risk of demagnetization was examined and discussed.

The performed investigations have shown that the LSPMSM reclosing is highly risky in terms of the permanent magnet demagnetization. The presented studies show also that one of the crucial factors demonstrating a significant impact on demagnetization is the resistance of the rotor cage winding. It has been shown that increasing the value of the resistance of the cage winding leads to the weakening of its shielding effect, whereby the motor can be permanently damaged.

If during the design process of the motor one would like to increase the resistance of the rotor cage in order to increase the starting torque or decrease the starting current, the risk of magnet demagnetization during the motor reclosing should be examined. The minimum cage resistance should ensure the proper screening of the permanent magnets also in such emergency operating conditions.

The calculations were carried out using resources provided by the Wroclaw Centre for Networking and Supercomputing (http://wcss.pl), grant No. 400.

References

[1] Kang G.-H., Hur J., Nam H., Hong J.-P., Kim G.T., *Analysis of Irreversible Magnet Demagnetization in Line-Start Motors Based on the Finite-Element Method*, IEEE Transactions on Magnetics, vol. 39, no. 3 (2003).

[2] Barański M., Szeląg W., Jędryczka C., *Influence of temperature on partial demagnetization of the permanent magnets during starting process of Line Start Permanent Magnet Synchronous Motor*, International Symposium on Electrical Machines, SME, Poland (2017).

[3] Yingli L., Zhiqiang L., Mingji L., Lifang Z., *Analysis on Fast Reclosing of Line Start Permanent Magnet Motor with Time-Stepping Finite Element Method*, Proceedings of the 11th International Conference on Electrical Machines and Systems, ICEMS, pp. 3257–3261 (2008).

[4] Ugale R.T., Nagabhushanrao V., Chaudhari B.N., Bhasme N.R., *Behavior of Line Start Permanent Magnet Synchronous Motor under Short Interruptions*, 2008 Joint International Conference on Power System Technology POWERCON and IEEE Power India Conference, POWERCON (2008).

[5] Lu W.-F., Zhao H.-S., Liu S., *Demagnetization Conditions Comparison for Line-start Permanent Magnet Synchronous Motors*, 17th International Conference on Electrical Machines and Systems (ICEMS), Hangzhou, China, Oct. 22–25 (2014).

[6] Behbahanifard H., Sadoughi A., *Line Start Permanent Magnet Synchronous Motor Performance and Design: a Review*, Journal of World's Electrical Engineering and Technology, vol. 4, no. 2, pp. 58–66, Dec. 25 (2015).

[7] Isfahani A.H., Vaez-Zadeh S., *Line start permanent magnet synchronous motors: challenges and opportunities*, Energy, vol. 34, no. 11, pp. 1755–1763 (2009).

[8] Barański M., Szeląg W., Lyskawiński W., *An analysis of a start-up process in LSPMSMs with aluminum and copper rotor bars considering the coupling of electromagnetic and thermal phenomena*, Archives of Elecrical Engineering, vol. 68, no. 4, pp. 933–946 (2019).

[9] Tian M., Wang X., Wang D., Zhao W., Li Ch., *A Novel Line-Start Permanent Magnet Synchronous Motor wit 6/8 Pole Changing Stator Winding*, IEEE Transactions on Energy Conversion, vol. 33, no. 3, pp. 1064–1074 (2018).

[10] Ershad N.F., Mirsalim M., Aliabad A.D., *Line-start permanent magnet motors: Proper design for pole-changing starting method*, IET Electric Power Applications, vol. 7, no. 6, pp. 470–476 (2012).

[11] Jędryczka C., Wojciechowski R.M., Demenko A., *Finite element analysis of the asynchronous torque in LSPMSM with non-symmetrical squirrel cage winding*, International Jorunalist of Applied Electromagnetics and Mechanics (IJAEM), vol. 46, no. 2, pp. 367–373 (2014).